Formation of stationary localized states due to nonlinear impurities using the discrete nonlinear Schrödinger equation

B. C. Gupta and K. Kundu
Institute of Physics, Bhubaneswar, 751 005, India
(Received 18 June 1996)

The discrete nonlinear Schrödinger equation is used to study the formation of stationary localized states due to a single nonlinear impurity in a Caley tree and a dimeric nonlinear impurity in the one-dimensional system. The rotational nonlinear impurity and the impurity of the form $-\chi|C|^{\sigma}$ where σ is arbitrary, and χ is the nonlinearity parameter are considered. Furthermore, $|C|$ represents the absolute value of the amplitude. Altogether four cases are studied. The usual Green's-function approach and the ansatz approach are coherently blended to obtain phase diagrams showing regions of different number of states in the parameter space. Equations of critical lines separating various regions in phase diagrams are derived analytically. For the dimeric problem with the impurity $-\chi|C|^{\sigma}$, three values of $|\chi_{cr}|$, namely, $|\chi_{cr}|=2$, at $\sigma=0$ and $|\chi_{cr}|=1$ and 8/3 for $\sigma=2$ are obtained. The last two values are lower than the existing values. The energy of the states as a function of parameters is also obtained. A model derivation of the impurities is presented. The implication of our results in relation to disordered systems comprising nonlinear impurities and perfect sites is discussed. [S0163-1829(97)07201-9]

I. INTRODUCTION

The discrete nonlinear Schrödinger equation (DNLSE) is a set of N coupled differential equations,

$$i\frac{dC_m}{dt}=-\chi_m f_m(|C_m|)C_m+V_{m,m+1}C_{m+1}+V_{m,m-1}C_{m-1},$$

where

$$V_{m,m+1}=V^{\star}_{m+1,m}, \quad \text{and} \quad m=1,2,3,\ldots,N. \tag{1}$$

In Eq. (1) the nonlinearity appears through functions $f_m(|C_m|)$, and χ_m is the nonlinearity parameter associated with the mth grid point. Since, $\Sigma_m|C_m|^2$ is brought to unity by choosing appropriate initial conditions, $|C_m|^2$ can be interpreted as the probability of finding a particle at the mth grid point. One way to derive this set of equations is to couple in the adiabatic approximation the vibration of masses at the lattice points of a lattice of N sites to the motion of a quasiparticle in the same lattice. The motion of the quasiparticle is described, however, in the framework of a tight binding Hamiltonian. The same type of equation can also be obtained by nonlinear coupling of anharmonic oscillators through both positions and momenta of the oscillators.[1–13] The set of equations, thus derived, are called discrete self–trapping equation (DST's). These equations also possess a constant of motion analogous to $\Sigma_m|C_m|^2$ in the DNLSE. In fact, both the DST and the DNLSE contain the same number of constants of motion.

An analytical solution of Eq. (1) in general is not known. However, nonlinear quantum dimers, which are two-site systems with the nonlinearity either in both the site energies or in one of them, can be solved analytically for any arbitrary initial condition. From analytical solutions a self-trapping transition is found in this model. The trapping of hydrogen ions around oxygen atoms in metal hydrides and the energy transport from the absorption center to the reaction center in a photosynthetic unit have been modeled by an effective quantum nonlinear dimer.[14–26] A nonlinear dimer analysis has also been applied to several experimental situations, like neutron scattering of hydrogen atoms trapped at impurity sites.[27,28]

The self-trapping of a quasiparticle at a nonlinear site in a perfect lattice containing a single nonlinear impurity has been studied. In the analysis, $f(|C_m|)$ was taken to be $|C_m|^2$. The critical value of the nonlinear parameter χ for the self-trapping is found to increase with increasing dimension.[29] It has also been shown that near the self–trapping transition the dynamics of the quasiparticle is mostly confined to the few near neighbors.[30] An interesting experimental example in this context is the observation that trapped hydrogen atoms in metals like Nb move among sites in the neighborhood of impurity atoms such as oxygen.[15,27,28] A self-trapping transition has also been obtained in systems where a nonlinear cluster is embedded in a perfect lattice. In fact, two types of transitions are obtained, with the cluster-trapping transition preceding the self-trapping transition.[31]

Another important feature of this type of nonlinear equation is that they can yield stationary localized (SL) states and solitonlike solutions. However, the presence of disorder or aperiodicity either in site energies or in nonlinearity parameters is needed for this purpose. For example, the Ablowitz-Ladik-like equation[32–38] can yield both localized and solitonlike solutions in the presence of disorder in static site energies. Similarly, the DNLSE can produce a solitonlike solution if any aperiodicity is present in the static site energies.[39] The effect of disorder in the static site energies, in the nonlinear parameters, and in both of these on the solution of the DNLSE has also been studied by numerical integrations. One also finds solitonlike solutions in this case. It has also been shown that the presence of nonlinear impurities in the absence of any disorder in the static site energies can

produce SL states in one dimension. The first study was made using the Green's-function approach, and the authors considered $f(|C_m|) = |C_m|^2$.[40] Furthermore, some cursory discussion on the two and more nonlinear impurities has been presented. Later, the one-nonlinear-impurity case has been generalized by taking $f(|C_m|)=|C_m|^\sigma$, and the formation of SL states is studied in one, two, and three dimensions.[41–43]

It is obvious from the above discussion that for a complete understanding of the single-nonlinear-impurity problem the effect of increasing of connections on the formation of SL states in the DNLSE needs further consideration. Thus, we plan to study the formation of SL states in the Caley tree in the presence of a single nonlinear impurity. Along with $f(|C_m|) = |C_m|^\sigma$, the effect of a more generalized nonlinearity impurity (like the rotational nonlinear impurity) also needs consideration. Furthermore, a thorough understanding of the nonlinear dimer problem in relation to SL states is required. This is a partial requirement to understand the effect of disorder in nonlinearity parameters in solutions of the DNLSE. Thus here we study in substantial detail the phase diagram of SL states due to the presence of a nonlinear dimer in the perfect one-dimensional chain. In this connection we also synthesize the original Green's-function approach and the ansatz approach.[40,41] Finally, we present a logical derivation of the DNLSE with $f(|C_m|) = |C_m|^\sigma$, by generalizing the potential of the nonlinear pendulum. To the best of our knowledge no such attempt has been made in this direction.

The organization of the paper is as follows. In Sec. II we consider a nonlinear impurity of the form $-\chi|C|^\sigma$ embedded in a Caley tree. We next consider in Sec. III a rotational nonlinear impurity in the Caley tree. In Sec. IV we deal with a dimeric nonlinear impurity in a one-dimensional system. The impurity is, of course, of the form $-\chi|C|^\sigma$. A similar problem with the rotational nonlinear impurity is considered in Sec. V. Section VI deals with a model derivation of the DNLSE considered here. Finally we conclude our paper by highlighting the major features and the importance of our results in understanding the behavior of disordered systems made up of nonlinear impurities and perfect sites.

II. SINGLE NONLINEAR IMPURITY OF THE FORM $-\chi|\,C\,|^\sigma$ IN A CALEY TREE

We consider a Caley tree with the coordination number, Z. Its connectivity is, therefore $K=Z-1$. We set a nonlinear impurity at a site and call it the zeroth site. Furthermore, here we consider $f_0(|C_0|) = |C_0|^\sigma$ where $\sigma\geqslant 0$. Now, from this site, Z branches will emerge. Again, from each of these branches K branches will emerge. So the number of points in the nth generation (or nth shell) is $ZK^{(n-1)}$. From any point in the nth shell a quasiparticle can move either to K points in the $(n+1)$th shell or to a point in the $(n-1)$-th shell if $n\geqslant 1$. Of course, we are considering only nearest-neighbor hopping with a real hopping element. So, if the nearest-neighbor hopping element is the same for all sites, every point in a given shell will show an identical time evolution of the probability amplitude of the quasi-particle. Thus the set of equations that describes the time evolution of the probability amplitude in the present model is[44]

$$i\frac{dC_n}{dt}=KC_{n+1}+C_{n-1}, \quad n\geqslant 1 \tag{2}$$

$$i\frac{dC_0}{dt}=-\widetilde{\chi}|C_0|^\sigma C_0+ZC_1, \quad n=0. \tag{3}$$

Furthermore, we have

$$|C_0(t)|^2+\frac{Z}{K}\sum_{n=1}^{\infty}K^n|C_n(t)|^2=1. \tag{4}$$

Since we are interested here in SL states, we write $C_n(t) = \exp(-i\widetilde{E}t)a_n$. After introducing this form of $C_n(t)$ in Eqs. (2) and (3), we make the following transformations: (i) $a_n=K^{-n/2}\phi_n$, (ii) E = $\widetilde{E}/\sqrt{K}$, and (iii) $\chi=\widetilde{\chi}/\sqrt{K}$. With these transformations, we finally obtain

$$E\phi_n=\phi_{n+1}+\phi_{n-1}, \quad n\geqslant 1, \tag{5}$$

$$E\phi_0=-\chi|\phi_0|^\sigma\phi_0+\frac{Z}{K}\phi_1, \quad n=0, \tag{6}$$

and

$$|\phi_0|^2+\frac{Z}{K}\sum_{n=1}^{\infty}|\phi_n|^2=1. \tag{7}$$

After some standard algebra for $|E|>2$,[32] from Eqs. (5) and (6) we obtain

$$\frac{\phi_n}{\phi_0}=\frac{E-\chi K|\phi_0|^\sigma}{Z}G^0_{n,0}(E)-G^0_{n+1,0}(E), \tag{8}$$

where $G_{n,0}(E)=[\mathrm{sgn}(E)]^{n+1}\ G^0_{0,0}(|E|)\ \eta^n$, and sgn$(E)$ denotes the signature of E. We also have $\eta=(|E|-\sqrt{E^2-4})/2$. So $0\leqslant\eta\leqslant 1$. For $G^0_{0,0}(|E|)$, we have

$$G_{0,0}(|E|)=\frac{1}{\sqrt{E^2-4}}=\frac{\eta}{1-\eta^2}\,. \tag{9}$$

Eq. (8) for $n = 0$ yields

$$1-\frac{EG^0_{0,0}(E)}{Z}+G^0_{1,0}(E)=-\frac{\chi K}{Z}|\phi_0|^\sigma G^0_{0,0}(E). \tag{10}$$

So the energy of SL states is obtained from solution of Eq. (10). We further note that the left-hand side of Eq. (10) is independent of the sign of E. On the other hand, to keep the sign unchanged on the right-hand side of Eq. (10), a simultaneous change of the signs of E and χ is required. Equation (10), when written in terms of η, assumes the form

$$\frac{K}{\eta}-\eta=-\chi K|\phi_0|^\sigma\mathrm{sgn}(E). \tag{11}$$

Similarly, Eq. (8), after some simple algebra, yields, for $n\geqslant 1$,

$$\phi_n=\phi_0\eta^n. \tag{12}$$

Now introducing Eq. (12) into Eq. (7), we obtain

$$\eta^2=\frac{K(1-|\phi_0|^2)}{K+|\phi_0|^2}\,. \tag{13}$$

Using Eq. (13), we eliminate η from Eq. (11), to obtain the equation for $|\phi_0|$. This in turn yields

$$\frac{4}{\tilde{\chi}^2}=|\phi_0|^{2\sigma}\frac{(K+1)^2-((K-1)+2|\phi_0|^2)^2}{(K-1+2|\phi_0|^2)^2}\,. \tag{14}$$

For $K=1$, Eq. (14) then gives

$$\frac{4}{\chi^2}=|\phi_0|^{2(\sigma-2)}(1-|\phi_0|^4), \tag{15}$$

and this equation has already been obtained.[41] We again note that $|\phi_0|^2\leqslant 1$. The energy (E) of SL states is

$$E=-\mathrm{sgn}(\chi)\left(\eta+\frac{1}{\eta}\right)$$

$$=-\mathrm{sgn}(\chi)\frac{(2K-(K-1)|\phi_0|^2)^2}{\sqrt{K}\sqrt{(K+1)^2-((K-1)+|\phi_0|^2)^2}}. \tag{16}$$

Equation (16) can be derived using Eqs. (13) and (14). We note that, for $\sigma=0$, Eq. (16) in conjunction with Eq. (14) yields

$$E=-\mathrm{sgn}(\chi)\left[-\frac{|\chi|(K-1)}{2}+\frac{K+1}{2\sqrt{K}}\sqrt{\chi^2K+4}\right]. \tag{17}$$

Equation (17) yields the correct result for a single linear impurity in a one-dimensional perfect system. We also see from Eq. (16) that, for $K=1$, $E=-\mathrm{sgn}(\chi)|\tilde{\chi}||\phi_0|^{\sigma-2}$. Then, for $\sigma=2$, $|E|=|\tilde{\chi}|$. Inasmuch as the minimum absolute value of the energy of a SL state is $2+$, the critical value of $|\chi|$, i.e., $|\tilde{\chi}_{\mathrm{cr}}|=2$. Above this value of $|\tilde{\chi}|$, two SL states are obtained.[41]

We numerically solve Eq. (14) for $|\phi_0|$ as a function of χ and σ. If $|\phi_0|\leqslant 1$, we obtain an admissible solution. Number of such solutions are the number of SL states in the system. We then calculate the energy of the SL states using Eq. (16). The phase diagram for SL states and energies of these states as a function of χ and σ are shown in Figs. 1 and 2 for $K=1$, 2, 3, and 10 respectively. We note that for $\sigma=0$ we have the standard Anderson localization problem. To obtain a localized eigenstate in a Caley tree of connectivity K, the condition $|\tilde{\chi}_{\mathrm{cr}}|\geqslant(K-1)/\sqrt{K}$ has to be satisfied. This can be obtained from Eq. (14) by setting $|\phi_0|^2=0$, and also from Eq. (17) by setting $|E|=2$. This is also obtained in our numerical analysis, as shown in Fig. 1. For $K=1$, there are three regimes. When $\sigma\leqslant 2$, there is always one SL state for $|\chi|>0$. For $\sigma\geqslant 2$, there is a critical value of χ $(|\chi_{\mathrm{cr}}|)$ for each σ (represented by a solid curve), below which no SL state appears, but above it two SL states ensue. On the other hand, for $K>1$, we find that for any value of $\sigma>0$, there is a $|\chi_{\mathrm{cr}}|$ below which no SL state appears, contrary to the $K=1$ case. But for $|\chi|>|\chi_{\mathrm{cr}}|$, we obtain two SL states. So there is a critical line (dashed line for $K=2$, dotted line for $K=3$, dot-dashed line for $K=10$ in Fig. 1.) in the (χ, σ) plane which separates the no-SL state region and the region containing two SL states. If one approaches the critical line from above for any σ, two distinct SL states merge on the critical line, and below that line they disappear. As we increase K, the separation between critical lines for any σ decreases, as shown in Fig. 1. So, $|\chi_{\mathrm{cr}}|$ becomes virtually independent of the connectivity for very large K. For the energy diagram (see Fig. 2) we have taken $\sigma=1$. We see that for $K=1$ the energy of the SL state increases with χ. This implies that localization becomes stronger for larger $|\chi|$. On the other hand for $K=2$, 3, and 10 i.e., for $K>1$, one of the two SL states increases with $|\chi|$. This corresponds to strong localization for large $|\chi|$. The energy of the other SL state goes toward the appropriate band-edge energy. This corresponds to weak localization for large $|\chi|$.

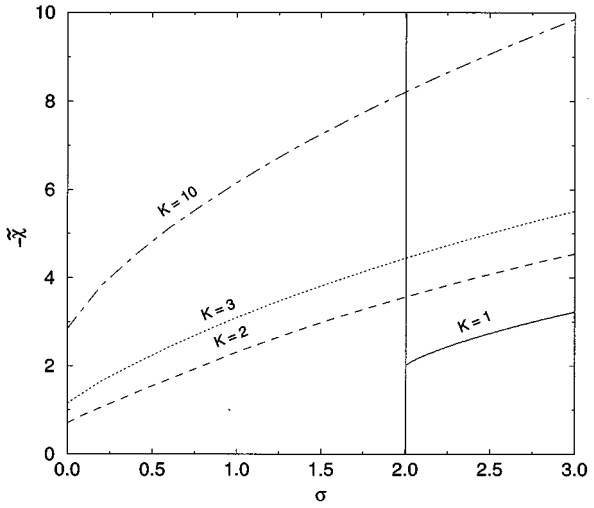

FIG. 1. Critical value of nonlinearity (χ_{cr}) separating the no-SL-state region from the two-SL-state region is plotted as a function of σ for Caley trees having $K=1$ (solid line), $K=2$, (dashed line), $K=3$ (dotted line), and $K=10$ (dot-dashed line). There is one nonlinear impurity in the Caley tree of the form $-\chi|C|^{\sigma}$.

We now present analytical results in favor of our numerical results. The relevant equation for this purpose is Eq. (14).

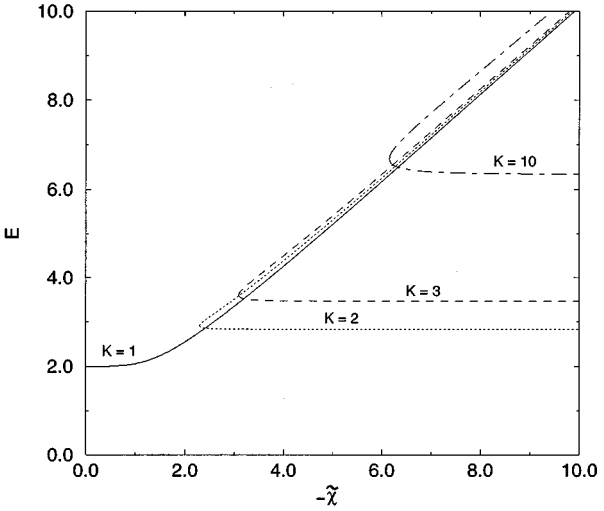

FIG. 2. The energy of SL states shown in Fig. 1 for $\sigma=1$ is plotted as a function of the nonlinearity parameter (χ) for the Caley tree. The solid curve is for $K=1$, the dotted curve is for $K=2$, the dashed curve is for $K=3$, and the dot-dashed curve is for $K=10$.

We denote the right-hand-side expression of Eq. (14) by $g_{K,\sigma}(A)$, where $A=|\phi_0|^2$. We note that for $\sigma>0$, $g_{K,\sigma}(0)=0=g_{K,\sigma}(1)$. We also have $g_{K,\sigma}(A)\geqslant 0$ for A in [0,1]. So there must be a maximum of this function with respect to A for A in [0,1]. For $\sigma=0$, this maximum occurs at $A=0$. If the value of the left-hand side of Eq. (14) lies above the maximum, no SL states will be obtained. However, for $(4/|\tilde{\chi}|^2)$ lying below the maximum, we shall obtain at least two SL states. Our numerical result suggests that $g_{K,\sigma}(A)$ has one maximum for A in [0,1]. So, by imposing the maximality condition on $g_{K,\sigma}(A)$ with respect to A, i.e., by setting $\partial g_{K,\sigma}(A)/\partial A=0$, we obtain

$$2\sigma A^3+3\sigma(K-1)A^2+[(K+1)^2+(K^2-4K+1)\sigma]A - \sigma K(K-1)=0\,. \tag{18}$$

Note that for $\sigma=0$, $A=0$. Furthermore, for $K=1$, we obtain $A=\sqrt{(\sigma-2)/\sigma}$. For $K>1$ and $\sigma>0$, Eq. (18) has only one real root RR given by

$$RR=\frac{(1-K)}{2}+\frac{3^{2/3}(\sigma-2)(K+1)^2+3^{1/3}D^2}{6\sqrt{\sigma}D} \tag{19}$$

where

$$D=[9\sqrt{\sigma}(K+1)^2(K-1)+\sqrt{3}(K+1)^2D_0]^{1/3} \tag{20}$$

and

$$D_0=\sqrt{(K+1)^2(2-\sigma)^3+27\sigma(K-1)^2}. \tag{21}$$

We emphasize that for all value of $\sigma>0$ and $K>1$, the RR is real and lies between 0 and 1. So the equation for the critical line in the (χ,σ) plane separating the no-state and the two-state regions is

$$|\chi_{\rm cr}|=\frac{2}{\sqrt{K}\sqrt{g_{K,\sigma}(\mathrm{RR})}}. \tag{22}$$

We now analyze the case of $K=1$ along the same line. The relevant equation is Eq. (15), in which the right-hand side will be denoted by $g_\sigma(A)$. Inasmuch as $0\leqslant A\leqslant 1$ the domain of $g_\sigma(A)$ is $[0,\infty]$ if $\sigma<2$. So, for $\sigma<2$, the line y = const $=(4/\chi^2)$ always intersects the curve $g_\sigma(A)$ at a single point. This will happen even if $|\chi|$ is infinitesimally small. So for $\sigma<2$ we shall always obtain one and only one SL state if $|\chi|>0$. Precisely this is obtained in Ref. 41. If $\sigma>2$, $g_\sigma(0)=0=g_\sigma(1)$. Furthermore, $g_\sigma(A)$ is positive semidefinite for A in [0, 1]. So there must be at least one maximum for A in [0, 1]. We also note that for $\sigma=2$, the maximum of $g_\sigma(A)$ occurs at $A=0$. Therefore, for $K=1$ and $\sigma=0$, applying the same analysis we obtain $|\chi_{\rm cr}|=2$, below which there is no SL state and above which there is one SL state. Furthermore, it can be shown from Eq. (15) by maximizing $g_\sigma(A)$ that $|\chi_{\rm cr}|$ separating the no-state and two-state regions for $\sigma>2$ is

$$|\chi_{\rm cr}|=\frac{\sqrt{2}\,\sigma^{\sigma/4}}{(\sigma-2)^{(\sigma-2)/4}}. \tag{23}$$

This expression for $|\chi_{\rm cr}|$ has been mentioned[41] without any derivation.

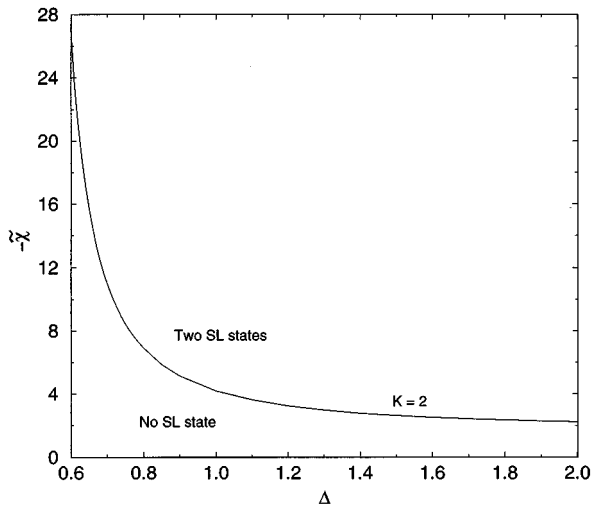

FIG. 3. The phase diagram for the Caley tree with a single rotational nonlinear impurity showing the number of SL states as a function of nonlinearity parameter (χ) and the parameter Δ. In this case the connectivity of the Caley tree, $K=2$.

III. SINGLE-ROTATIONAL-NONLINEAR IMPURITY IN A CALEY TREE

Here we consider the case where $f(|C_0|)=|C_0|/(\sqrt{1+(\chi/\Delta)^2|C_0|^2})$. The origin of this particular form of nonlinearity was discussed in Ref. 45. For this case, from the appropriate version of Eq. (10), for $|\phi_0|^2=A$ we obtain

$$A^4+(K-1)A^3+PA^2+Q=0, \tag{24}$$

where

$$P=\frac{4-\chi^2\left(K^2-\left(\frac{K-1}{\Delta}\right)^2\right)}{\chi^2\left(\frac{4}{\Delta^2}+K\right)} \tag{25}$$

and

$$Q=(K-1)^2\Big/\left[\chi^2\left(\frac{4}{\Delta^2}+K\right)\right]. \tag{26}$$

For $K=1$, that is for a one-dimensional system, we find, from Eq. (24),

$$A=\frac{\sqrt{\chi^2-4}}{\sqrt{\chi^2+\Delta^2}}\left|\frac{\Delta}{\chi}\right|. \tag{27}$$

So if $|\chi|>2$, one and only one SL state will be obtained. Furthermore, the energy (E) of this SL state is

$$E=\pm|\chi|\left(\frac{4+\Delta^2}{\chi^2+\Delta^2}\right)^{1/2}. \tag{28}$$

However, $K>1$, the analytical calculation of the energy of the SL state is quite prohibitory. So we examine the case for $K=2$. Our results are shown in Fig. 3. We again find two regions. In the lower region we find no SL state. On the other hand, in the upper region there are two SL states. The line

separating these regions contains one SL state. We find that, for $|\Delta|\to 0$, $|\chi_{cr}|\to\infty$. This should be expected. Another interesting feature is that $|\chi_{cr}|$ reduces with increasing $|\Delta|$. For small value of $|\Delta|$, the fall in $|\chi_{cr}|$ is quite sharp with increasing $|\Delta|$.

IV. NONLINEAR DIMER IMPURITY IN A ONE-DIMENSIONAL PERFECT CHAIN: IMPURITY OF $-\chi|\ C\ |^{\sigma}$ TYPE

Two consecutive sites occupied by nonlinear impurities are labeled as zeroth and first sites, respectively. Here we consider, $\chi_0 f_0(|C_0)|)=\chi|C_0|^{\sigma}$ and $\chi_1 f(|C_1|)=\chi|C_1|^{\sigma}$. All other χ_m are set to zero. All $V_{n,n+1}$ in Eq. (1) are set to unity. Since we are looking for SL states, we set $C_n(t)=\phi_n\exp(-iEt)$ in the appropriate version of Eq. (1). From the set of equations thus obtained we solve for ϕ_n by the standard procedure.[32] Consequently, we obtain

$$\phi_n=G^0_{n,0}(E)\,\epsilon_0\phi_0+G^0_{n,1}(E)\,\epsilon_1\phi_1\,. \tag{29}$$

In Eq. (29), for the purpose of generality, we define $\epsilon_0=-\chi|\phi_0|^{\sigma}$ and $\epsilon_1=-\chi|\phi_1|^{\sigma}$. Furthermore, for $n=0$ and $n=1$, Eq. (29) yields

$$\phi_0=G^0_{0,0}(E)\,\epsilon_0\phi_0+G^0_{0,1}(E)\,\epsilon_1\phi_1 \tag{30}$$

and

$$\phi_1=G^0_{1,0}(E)\,\epsilon_0\phi_0+G^0_{1,1}(E)\,\epsilon_1\phi_1\,. \tag{31}$$

We note that $G^0_{n,m}(|E|)$ has been defined by Eq. (9). After some simple algebra it can be shown with the help of Eqs. (30) and (31) that

$$\phi_n=(\mathrm{sgn}(E)\,\eta)^{n-1}\phi_1\,,\quad n>1, \tag{32}$$

$$\phi_{-|n|}=(\mathrm{sgn}(E)\,\eta)^{|n|}\phi_0\,,\quad |n|>0, \tag{33}$$

where $0\leqslant\eta\leqslant 1$ as was defined in Sec. II. We further note that the form of ϕ_n given by Eqs. (32) and (33) is independent of the form of ϵ_0 and ϵ_1. Since we must have $\Sigma_{-\infty}^{\infty}|\phi_n|^2=1$, using Eqs. (32) and (33) we find that

$$|\phi_0|^2+|\phi_1|^2=1-\eta^2. \tag{34}$$

When ϵ_0 and ϵ_1 are linear impurities, from Eqs. (30) and (31) we obtain

$$E_{\pm}=\frac{\epsilon_0\epsilon_1(\epsilon_0+\epsilon_1)\pm|2-\epsilon_0\epsilon_1|\sqrt{(\epsilon_0-\epsilon_1)^2+4}}{2(\epsilon_0\epsilon_1-1)}, \tag{35}$$

where $E_{\pm}$ denotes the energy of the SL state. We note that for $\epsilon_0=\epsilon_1>2$, two SL states appear above the band. The situation reverses for $\epsilon_0=\epsilon_1<-2$. Furthermore, for $\epsilon_0=\epsilon_1\to 0$, we obtain $E_{\pm}=\pm 2$. In other words, we obtain one of the band-edge states. These are consistent with established results,[46] but the exact form of the solution is not presented there. In the present model we have $\epsilon_0=\epsilon_1=-\chi$ for $\sigma=0$. On the other hand, since $|\phi_0|,|\phi_1|<1$, for a finite χ, if $\sigma\to\infty$, we obtain $\epsilon_0=\epsilon_1\to 0$. General solutions of the nonlinear dimer impurity problem are expected to show these asymptotic behaviors. It should be noted in this context that for a single nonlinear impurity this continuity has been rigorously established.[41]

We now consider the case of our nonlinear dimer. We have three equations, namely, (30), and (31), and (34). So, if ϕ_0 and ϕ_1 are fully complex quantities, for the problem to be well posed, we must have $\phi_1=\phi_0^{\star}$. Otherwise, the problem is well posed. From Eqs. (30) and (31), we obtain

$$Y^{\sigma+2}=\left|\frac{1}{1+X}\right|, \tag{36}$$

where

$$Y=\left|\frac{\phi_1}{\phi_0}\right| \tag{37}$$

and

$$X=\frac{\chi G^0_{0,0}(E)|\phi_0|^{\sigma}(Y^{\sigma}-1)}{1+\chi G^0_{0,0}(E)|\phi_0|^{\sigma}}. \tag{38}$$

It is to be noted that, for $|\phi_0|=|\phi_1|$, Eq. (36) becomes an identity. Consider now the case where $\chi G^0_{0,0}(E)>0$. This limit can be obtained either by (i) $\chi>0$, $E>2$ or by (ii) $\chi<0$, $E<-2$. It is easy to see that if $Y\neq 1$, Eq. (36) is not satisfied. So the solution in this limit is $|\phi_0|=|\phi_1|$. Since these quantities can be taken as real, we have $\phi_0=\pm\phi_1$. However, it can be trivially shown either from Eqs. (30) or (31) that no SL states will be obtained in this case. Consider next the other limit where $\chi G^0_{0,0}(E)<0$. To achieve this limit we need either (i) $\chi<0$, $E>2$ or (ii) $\chi>0$, $E<-2$. Now it can be easily shown that if both $D_0=1-|\chi G^0_{0,0}(E)||\phi_0|^{\sigma}<0$ and $D_1=1-|\chi G^0_{0,0}(E)||\phi_1|^{\sigma}<0$, the solution of Eq. (36) is, again $|\phi_0|=|\phi_1|$. Note further that if $Y>1$ is a solution of Eq. (36), $Y<1$ should also be a solution of Eq. (36) [see, for example, Eq. (35)]. So, any constraint on D_0 will imply a similar constraint on D_1, and vice versa. On the other hand, we may have $|\phi_0|\neq|\phi_1|$ if $D_0>0$, and, consequently, also $D_1>0$. We again consider Eq. (30), which for $\chi G^0_{0,0}(E)<0$ is

$$1-|\chi G^0_{0,0}(E)||\phi_0|^{\sigma}=|\chi G^0_{0,0}(E)||\phi_1|^{\sigma}\eta\ \mathrm{sgn}(E)\left(\frac{\phi_1}{\phi_0}\right). \tag{39}$$

We can also consider the equation for ϕ_1 [Eq. (31)]. Both equations will yield the same conclusion. It is easy to see that for $E>2$, Eq. (39) tells that (ϕ_1/ϕ_0) must be positive. On the other hand, for $E<-2$, (ϕ_1/ϕ_0) should be negative. This result, coupled with the formula for ϕ_n [Eqs. (32) and (33)], suggests that SL states for $D_0>0$ either have no nodes for $E>2$, or have N (the number of sites in the lattice) nodes for $E<-2$. We further note that band-edge states in the perfect system have these characteristics. In the case of the linear eigenvalue problem, we know that there will be only one SL state in this limit. This SL state will evolve from one of the band-edge states. Since here all we are dealing with a nonlinear eigenvalue problem, it is in principle possible to have multiple permissible values of ϕ_0 and ϕ_1. In other words, we may obtain a set of states. We shall refer to this as a symmetric set. But all these SL states will contain the same number of nodes. Of course, a subset of these states will have $\phi_0=\phi_1$, and one state in this subset will survive for $\sigma=0$.

In the linear dimer impurity problem we also obtain another SL state. This state has either a node ($E>2$) through the dimer, or the node through the dimer disappears ($E<-2$). We should have the same situation with the nonlinear dimer, but instead of having one such state we may have a set of states, again with the same number of nodes. Since in the second set we must have $\phi_1/\phi_0 = -\mathrm{sgn}(E)|(\phi_1/\phi_0)|$, for this set to appear we need $D_0, D_1 < 0$. This, in turn implies that the second set of states should always have $|\phi_0| = |\phi_1|$. Thus, states where $\phi_0 = \phi_1$ in the first set together with states coming from this antisymmetric set, will constitute a major part of the phase diagram for SL states. This phase diagram will be discussed here. We also analyze if $\phi_0 \neq \phi_1$ is at all possible in the first set of SL states.

For $|\phi_0| = |\phi_1|$ from either Eq. (30) or (31), for $|E|>2$, we obtain

$$\eta_{\pm} = \frac{1}{|\chi||\phi_0|^{\sigma} \pm 1}\,. \tag{40}$$

For positive sign we need $\phi_1/\phi_0 = -\mathrm{sgn}(\chi) = \mathrm{sgn}(E)$, while for the other sign $\phi_1/\phi_0 = \mathrm{sgn}(\chi) = -\mathrm{sgn}(E)$. Furthermore, the equation for determining $|\phi_0|$ can be obtained from Eqs. (34) and (40). The required equation for $|\phi_0|$ is

$$(1-2|\phi_0|^2)(\chi|\phi_0|^{\sigma} \pm 1)^2 = 1, \tag{41}$$

and the energy of the SL state (E) is $E = \mathrm{sgn}(E)[\eta + (1/\eta)]$, $0 \leqslant \eta \leqslant 1$.

The phase diagram is obtained by analytical as well as numerical calculations (see Fig. 4). We first describe our numerical findings. Note that for $\sigma = 0$, we have one state for $|\chi|<2$ and then for $|\chi|>2$ second state appears. This agrees with established results.[46] On the other hand, we find that for $0 \leqslant \sigma \leqslant 2$ we find a regime (I) with one SL state (coming only from symmetric set). For all values of σ in this range there is a $|\chi_{cr}|$ which increases with increasing σ, shown the in figure by the dotted line. Two SL states exist along this line. Note further that one of these states comes from the antisymmetric set. Above this line we then have a regime (IV) where three SL states are obtained (one from the symmetric set and other two from the antisymmetric set).

We now consider the case where $\sigma>2$. We have a region (II) where no SL state exists. Note that a similar situation is also obtained for one nonlinear impurity case.[41] This region is bounded by a critical line along which one SL state exists (shown by the solid line in Fig. 4). This state comes from the symmetric set. Above this critical line we have a region (III) of two SL states. Furthermore, we never obtain more than two states from the symmetric set. This region of two states continues until we reach the critical line (shown by the dotted line in the Fig. 4) due to the antisymmetric set. Along this line we always have three SL states, and above this line we have a region (V) of four SL states. We also mention that $\sigma = 2$ is the special line. Along this line all transitions take place. For example, $|\chi_{cr}|$ at $\sigma = 2$, below which no SL state is obtained, is 1 (this is shown by the lower box along the $\sigma = 2$ line in the figure). The previously reported value of this $|\chi_{cr}|$ is 2, and this value is obtained from an approximate calculation.[40] Another $|\chi_{cr}|$ is found to be exactly 8, which comes from the antisymmetric set (this is shown by the upper box along the $\sigma = 2$ line in the figure). We also emphasize that the $\sigma = 2$ line is a line of continuity. The energy of states as a function χ in regions I and IV of Fig. 4 is shown in Fig. 5. We have taken $\sigma = 1$ for example to analyze this. In region I the energy of the state always increases with increasing $|\chi|$. In region IV, the energy of one of the two states belonging to the antisymmetric set decreases with in-

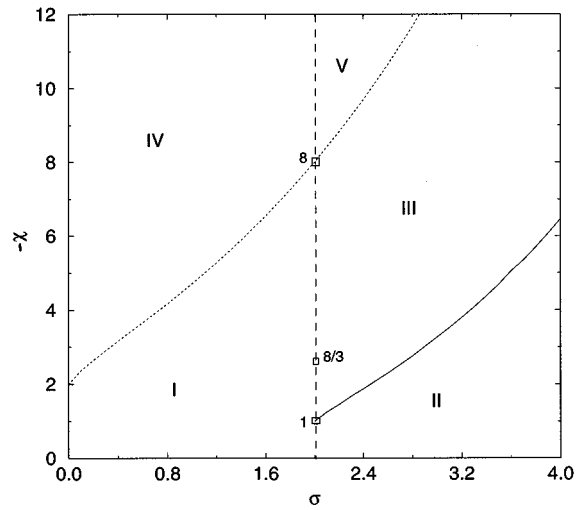

FIG. 4. The phase diagram for a perfect chain with a nonlinear dimer made up of impurities of the form $-\chi|C|^{\sigma}$. The figure shows regions containing different number of SL states in the (χ,σ) plane. There are one SL state in region I, no SL state in region II, two SL states in region III, three SL states in region IV and four SL states in region V. The solid $|\chi_{cr}|$ curve arises from the symmetric set and the dotted curve arises from the antisymmetric set. At $\sigma = 2$ three values of $|\chi_{cr}|$ exist. These points are shown by boxes. The upper box along the $\sigma = 2$ line corresponds to $\chi_{cr} = 8$, which comes from antisymmetric set (i.e., $\phi_0 = -\phi_1$). The lower box corresponds to $\chi_{cr} = 1$, which comes from symmetric set (i.e., $\phi_0 = \phi_1$). But the middle box corresponds to $\chi_{cr} = \frac{8}{3}$, and this appears for the case when $|\phi_0| \neq |\phi_1|$.

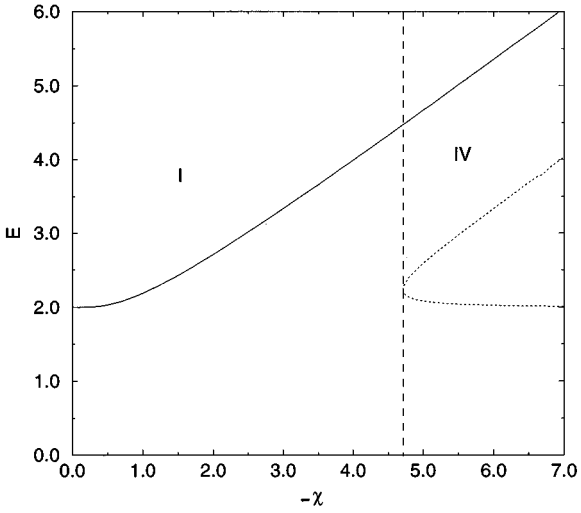

FIG. 5. The energy diagram of SL states as a function of χ at $\sigma = 1$, which corresponds to the regions I and IV of Fig. 4. The solid curve is due to the symmetric set, and the dotted curve is due to the antisymmetric set.

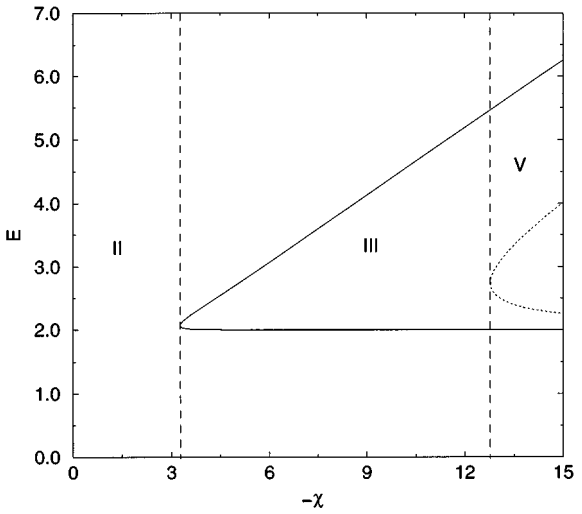

FIG. 6. The energy diagram for SL states as a function of χ at $\sigma = 3$, which corresponds to the regions II, III, and V in Fig. 4. The solid curve is due to the symmetric set and the dotted curve is due to the antisymmetric set. The dashed vertical lines touch the solid and dotted curves at the critical values of $|\chi|$.

creasing $|\chi|$, and it reduces asymptotically to $E=2$ (the band-edge state). The energy diagram in regions II, III, and V is shown in Fig. 6. In this case we have taken $\sigma=3$. The energy diagram also shows three distinct regions having no state, two states, and four states. Two consecutive regions are separated by critical lines where one and three states exist, respectively. We should note that the energy of one pair of states (one from the symmetric set and the other from the antisymmetric set) decreases asymptotically to $E=2$ (band edge state) with increasing $|\chi|$. The energy of other pair increases as $|\chi|$ increases.

We now provide analytical support for our numerical results. Since, here we are considering the case $|\phi_0|^2=|\phi_1|^2$, from Eq. (34) we obtain $|\phi_0|^2=(1-\eta^2)/2$. Then, from Eq. (40), we obtain

$$\frac{2^{\sigma/2}}{|\chi|}=\eta_{\pm}(1\mp\eta_{\pm})^{-1}(1-\eta_{\pm}^2)^{\sigma/2}. \tag{42}$$

In Eq. (42) the upper case sign is for the symmetric set, while the lower case sign represents the antisymmetric set. We first consider the symmetric case. We denote the right-hand side of Eq. (42) by $g_s(\sigma,\eta)$

$$g_s(\sigma,\eta)=\eta(1+\eta)^{(\sigma/2)}(1-\eta)^{(\sigma/2)-1}, \tag{43}$$

and η lies in [0, 1]. We further note that for $\sigma<2$, the domain of $g_s(\sigma,\eta)$ is $[0,\infty]$. So, by applying our analysis of one nonlinear impurity in a one-dimensional system, we obtain that, for $\sigma<2$, the system will produce one and only one SL state for $|\chi_{\rm cr}|>0$. In other words, in this limit $|\chi_{\rm cr}|=0$. This is precisely seen in our numerical calculation. On the other hand, for $\sigma>2$, $g_s(\sigma,0)=0=g_s(\sigma,1)$. Furthermore, $g_s(\sigma,\eta)$ is positive semidefinite for η in [0, 1]. This, in turn implies that there will be a regime where no SL state will exist. However, for $|\chi|$ exceeding some critical value $|\chi_{\rm cr}|$, we shall obtain at least two SL states. It is quite transparent from the form of $g_s(\sigma,\eta)$ that the function has only one maximum with respect to η in [0, 1]. Our numerical calculations also suggest that this is so. Therefore, there will be a no-SL-state region and a two-localized-state region separated by a line in the (χ,σ) plane. Furthermore, only one SL state will exist along this line. To obtain the equation for this line, we as usual maximize $g_s(\sigma,\eta)$ with respect to η. This then yields

$$\sigma\eta^2-\eta-1=0, \tag{44}$$

and the permissible solution for η, η_{ms} is

$$\eta_{ms}=\frac{1+\sqrt{1+4\sigma}}{2\sigma}. \tag{45}$$

Now from Eq. (43) we obtain, for $\sigma>2$,

$$|\chi_{\rm cr}|=\frac{2^{\sigma/2}}{g_s(\sigma,\eta_{ms})}. \tag{46}$$

For $\sigma=2$, $g_s(2,\eta)=2$ is the maximum permissible value of $g_s(2,\eta)$ for η in [0, 1]. Albeit this is not a true maximum of $g_s(\sigma,\eta)$, the left-hand side of Eq. (42) must attend this value to obtain a SL state. Hence for $\sigma=2$, $|\chi_{\rm cr}|=1$. Analytical continuation of Eq. (46) also yields this result.

For the antisymmetric case the relevant function to analyze is

$$g_a(\sigma,\eta)=\eta(1-\eta)^{\sigma/2}(1+\eta)^{(\sigma/2)-1}. \tag{47}$$

We note that for $\sigma>0$, $g_a(\sigma,0)=0=g_a(\sigma,1)$. The function is also positive semidefinite for η in [0, 1]. Hence there will be a maximum of $g_{(\sigma,\eta)}$ with respect to η for η in [0, 1]. It is obvious from the structure of $g_a(\sigma,\eta)$ that there is only one maximum. From these we conclude that there will be two regions, one having no SL state and the other containing two SL states. Again the line separating these regions will contain only one SL state. To obtain the equation of this line, we maximize $g_a(\sigma,\eta)$ with respect to η. We thus obtain

$$\sigma\eta^2+\eta-1=0, \tag{48}$$

and the permissible solution of η, η_{ma} is

$$\eta_{ma}=\frac{\sqrt{4\sigma+1}-1}{2\sigma}. \tag{49}$$

So, the equation for the $\chi_{\rm cr}$ line is

$$|\chi_{\rm cr}|=\frac{2^{(\sigma/2)}}{g_a(\sigma,\eta_{ma})}. \tag{50}$$

We again note that for $\sigma=2, \eta_{am}=1/2$ which in turn yields $g_a(\sigma,\eta_{am})=1/4$. Hence from Eq. (47) we obtain $|\chi_{\rm cr}|=8$. This is obtained from our numerical calculation. For $\sigma=0$, the maximum permissible value of $g_a(0,\eta)$ is 1/2, which occurs at $\eta=1$. Consequently from Eq. (50) we obtain $|\chi_{\rm cr}|=2$. This also agrees with the established result for static dimer impurities.[46] We further note that the analytical continuation of Eq. (50) also produce this result. We now note the following. (1) If $\sigma\to\infty$, $\eta_{ms}\sim\eta_{ma}=1/\sqrt{\sigma}$. This implies that two critical lines will approach each other as σ increases. (2) In contrast to the symmetric case, the antisymmetric case will have nonzero $|\chi_{\rm cr}|$ for all $\sigma(>0)$ separating

the no-SL-state and two-SL-state regimes. (3) The value of $|\chi_{cr}|$ for the antisymmetric case is greater than the corresponding value in the symmetric case if σ is finite. (4) For the antisymmetric case, there is no regime with one SL state except the critical line. This is again in contrast to the symmetric case, but quite similar to the Caley tree case.

We now consider the possibility of $\phi_0 \neq \phi_1$ in the region where D_0, $D_1 > 0$. Since $E > 2$, $-\chi > 0$, we are taking strictly χ positive to avoid complication. From the starting equation of ϕ_n, $n \in N$, we obtain

$$\chi(|\phi_0|^\sigma - |\phi_1|^\sigma) = \frac{\phi_0^2 - \phi_1^2}{\phi_1 \phi_0} \tag{51}$$

and

$$\eta = \frac{1}{\chi|\phi_0|^\sigma + \frac{\phi_1}{\phi_0}} = \frac{1}{\chi|\phi_1|^\sigma + \frac{\phi_0}{\phi_1}}. \tag{52}$$

Furthermore, we have Eq. (34). We emphasize that not only that ϕ_0 and ϕ_1 have the same sign, but that they are real quantities. For $\sigma = 2$, after some algebra we find that

$$\eta^3 - \eta + \frac{1}{\chi} = 0 \tag{53}$$

and

$$\beta = \frac{\phi_1}{\phi_0} = \frac{1 \pm \sqrt{1 - 4\eta^2}}{2\eta}. \tag{54}$$

Since β should be real, we must have $\eta < 1/2$. Then, from Eq. (53), we find $|\chi_{cr}| = 8/3$ for this case. This is shown by the middle box along $\sigma = 2$ line in Fig. 4. We emphasize that to the best of our knowledge this result has not been obtained before. So, along the $\sigma = 2$ line we have (i) $|\chi| < 1$, no SL state; (ii) $1 \leqslant |\chi| \leqslant 8/3$, one SL state; (iii) $8/3 < |\chi| < 8$, two SL states; (iv) $|\chi| = 8$, a point of three SL states and (v) $|\chi| > 8$, four SL states. Furthermore, where we have two or more SL states, one of the states has $\phi_0 \neq \phi_1$. This state appears for $|\chi_{cr}| \geqslant 8/3$. The case of $\sigma = 1$, 3, and 4 have also been examined. No SL state for $\phi_0 \neq \phi_1$ is found. It appears that $\sigma = 2$ is a very special case. Further analysis for arbitrary σ will be presented elsewhere. Before concluding this section we again point out that for $\sigma = 2$ and $|\chi| \geqslant 8$, of the four SL states, two states come from the antisymmetric set.

V. ROTATIONAL NONLINEAR DIMER IMPURITY IN A PERFECT CHAIN

We now consider the case where $f_m(|C_m|) = |C_m|^2/(\sqrt{1 + (\chi/\Delta)^2 |C_m|^4})$ for $m = 0$ and 1, and zero otherwise. In other words we have nonlinear dimer impurities made up of so-called rotational nonlinear impurities.[45] In this case $\phi_0 = \pm \phi_1$ also constitute a set of solutions. We focus our attention on this set. A more general case will be considered elsewhere. Here we have two cases, namely, the symmetric case, where $\phi_0 = \phi_1$, and the antisymmetric case otherwise. For the symmetric case from the appropriate version of Eq. (40), along with Eq. (34) we obtain

$$\frac{4\Delta^2}{\chi^2} = (1+\eta)^2[\Delta^2\eta^2 - (1-\eta)^2] = G_\Delta^+(\eta). \tag{55}$$

Since the left-hand side of Eq. (55) is always positive, we need $\eta \geqslant 1/(1+\Delta)$ but at the same time we need $\eta \leqslant 1$. So the condition on η is $1/(1+\Delta) \leqslant \eta \leqslant 1$. It is obvious that the constraint is met for $\Delta \geqslant 0$. On the other hand, $G_\Delta^+(1) = 4\Delta^2$. Since $G_\Delta^+(\eta)$ is monotonically increasing function of η for η in [0, 1], $4\Delta^2$ is the maximum permissible value of the function. So, for a SL state to appear we need $|\chi_{cr}| = 1$. Since there is only one intersection of a line $y = 4\Delta^2/\chi^2 = \text{const}$ with the curve $G_\Delta^+(\eta)$ for η in [0, 1] and $|\chi| > 1$, we shall always obtain one and only one SL state from the symmetric case if $|\chi| \geqslant |\chi_{cr}| = 1$.

For the antisymmetric case from the appropriate version of Eqs. (40) and (34) we obtain

$$\frac{4\Delta^2}{\chi^2} = (1-\eta)^2[\Delta^2\eta^2 - (1+\eta)^2] = G_\Delta^-(\eta). \tag{56}$$

Since $G_\Delta^-(\eta)$ should be positive semidefinite in the permissible interval of η not exceeding [0, 1], we need $\eta_{min} \geqslant 1/(\Delta - 1)$, since for $\eta \leqslant 1$, we must have $\Delta \geqslant 2$. We note now that $G_\Delta^-(1) = 0 = G_\Delta^-(\eta_{min})$. So, there must be at least one maximum of $G_\Delta^-(\eta)$ with respect to η. Imposing the condition of maximality on $G_\Delta^-(\eta)$ with respect to η, we obtain

$$\eta_{max} = \frac{\Delta^2 + 2}{2(\Delta^2 - 1)}. \tag{57}$$

It can be easily shown that $\eta_{max} \leqslant 1$. Furthermore $\eta_{max} < \eta_{min}$. Then by setting $\eta_{max} = \eta_{min} = 1/(\Delta - 1)$, we again find that $\Delta_{cr} = 2$. We also note that $G_\Delta^-(\eta)$ has only one allowed maximum for η in $[\eta_{min}, 1]$. Hence above this maximum we shall not obtain any SL state. On the other hand, for $4\Delta^2/\chi^2$ lying below this maximum, we shall obtain two SL states. The equation of the line separating these two regions is

$$|\chi_{cr}| = \frac{2\Delta}{\sqrt{G_\Delta^-(\eta_{max})}}. \tag{58}$$

We further note that Eqs. (56) and (57) in the limit $\Delta \to \infty$ yield $|\chi_{cr}| = 8$. This is expected.

In Fig. 7 we shown graphically the existence or nonexistence of SL states for the antisymmetric case, with $\Delta = 4$, for example. The plot of $G_\Delta^-(\eta)$ is shown as a dotted curve. Along with that we have superimposed the lines $y = 4\Delta^2/\chi^2$ for three values of χ as shown in figure. The line with $|\chi| = 11.313$ touches the maximum point of the dotted curve, and represents one SL state. So any line with $|\chi| < 11.313$ will not touch the dotted curve, and hence there are no SL states for $|\chi| < 11.313$ (for example the upper line is for $|\chi| = 9.65$). On the other hand, the lines with $|\chi| > 11.313$ will touch the line twice. Therefore there will exist two SL states for $|\chi| > 11.313$ (for example, the third line with $|\chi| = 14.61$). Therefore it is very transparent that for this case with $\Delta = 4$, $|\chi_{cr}| = 11.313$.

We next consider the full phase diagram obtained numerically. This is shown in Fig. 8. For $|\chi| < 1$ we have a no-state

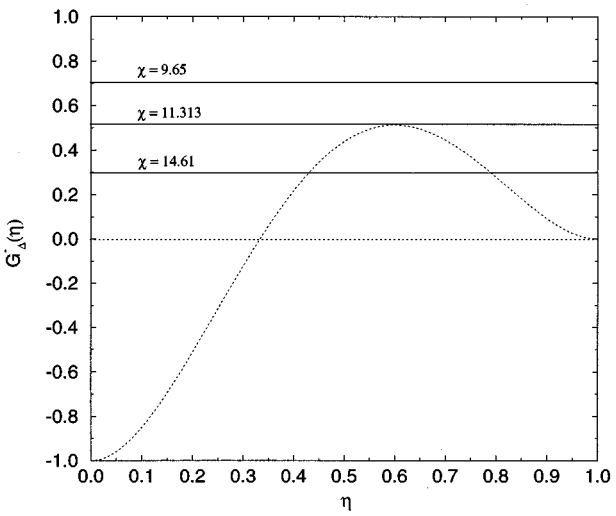

FIG. 7. The function $G_{\Delta}^{-}(\eta)$ is plotted as a function of η (dotted curve). The solid lines correspond to the $y=4\Delta^2/\chi^2$ for $|\chi| = 9.65$, 11.313, and 14.61, respectively. Here $\Delta=4$.

region for any Δ. For $|\chi|>1$ and $\Delta\leqslant 2$, we have a region where one SL state exists (coming from symmetric set). For $|\chi|>1$ and $\Delta>2$, we have two regions separated by a critical line (shown by solid line) in the (χ,Δ) plane. Above this critical line we have three SL states (one from symmetric set and other two from antisymmetric set) but below this line we have only one state (coming from the symmetric set). On the critical line only two SL states exist (one from the symmetric set and the other one from the antisymmetric set). The energy of SL states as a function of χ for $\Delta=4$ is shown in Fig. 9. It shows the typical behavior.

VI. MODEL DERIVATION OF THE DNLSE WITH GENERALIZED NONLINEARITIES

To start with, we consider a model potential $V(x)$ given by

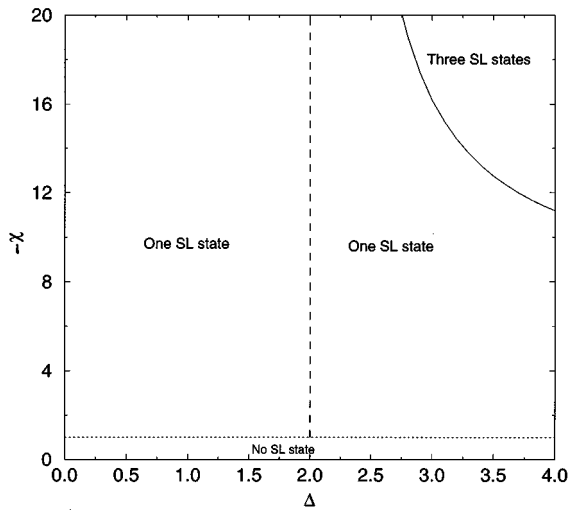

FIG. 8. The phase diagram for the perfect chain with a rotational nonlinear dimer impurity showing the number of SL states as a function of χ and Δ.

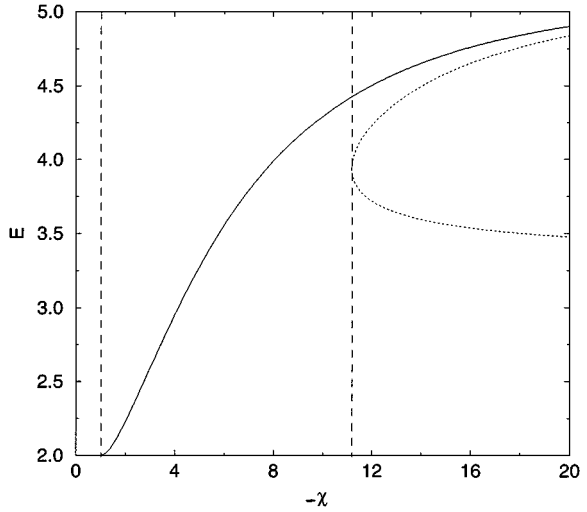

FIG. 9. The energy for SL states shown in Fig. 8 is plotted as a function of χ for $\Delta=4$.

$$V(x)=k\left[\frac{1-\cos(2\gamma x)}{4\gamma^2}\right]^d. \tag{59}$$

When $d = 1$, we obtain the potential for the nonlinear pendulum. We also know that such a system exhibits two types of motion, namely, libration and rotation. Two regions are separated by a critical line, called separatrix.[47] A similar situation also occurs for general d. When $d=\frac{1}{2}$, the periodic part of the potential is of sawtooth type, with kinks smoothed out. For $d>>1$, the periodic part is more like a repeated hard-wall potential. These are shown in Fig. 10. We further note that for $\gamma\rightarrow 0$, $V(x)\approx(k/2^d)|x|^{2d}$. For $d = 1$, we obtain the usual Hook spring. On the other hand, for general d the spring deviates from the Hookian behavior.

We consider next a Hamiltonian H given by

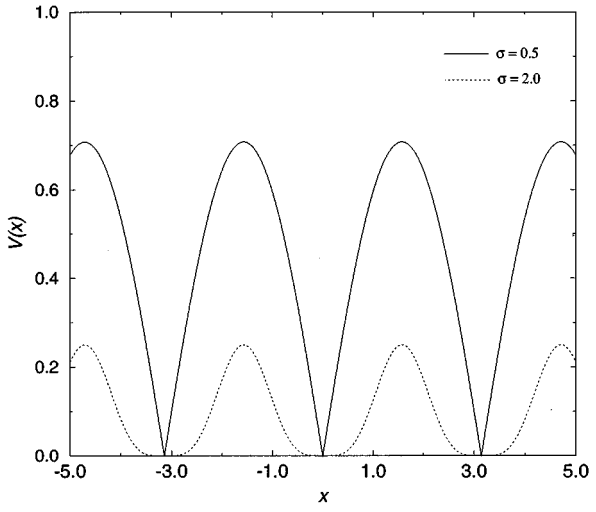

FIG. 10. The potential $V(x)=k([1-\cos(2\gamma x)]/4\gamma^2)^{\sigma}$ is plotted as a function of x. The solid curve is for $k=1,\gamma=1$, and $\sigma=0.5$, and the dotted one is for $k=1,\gamma=1$, and $\sigma=2$.

$$H=\frac{1}{2}\sum_{n=1}^{N}\left[\omega_n(x_n)|C_n|^2+(C_nC_{n+1}^{\star}+C_n^{\star}C_{n+1})\right]+\sum_{n=1}^{N}\left[\frac{p_n^2}{2m_n}+V_n(x_n)\right]=H_1+H_2. \tag{60}$$

By defining positions (Q_n) and momenta (P_n) by $Q_n=(C_n+C_n^{\star})/2$ and $P_n=i(C_n^{\star}-C_n)/2$ respectively, we find that

$$H_1=\frac{1}{2}\sum_n \omega_n(x_n)(P_n^2+Q_n^2)+\sum_n (P_nP_{n+1}+Q_nQ_{n+1}). \tag{61}$$

So H_1 can be said to define the dynamics of a superoscillator with $2N$ degrees of freedom. Furthermore, the frequency of the oscillator in a given direction is coupled to the motion of another oscillator defined by x_n.[7] On the other hand, we can replace $C_n(C_n^{\star})$ in H_1 by the annihilation (creation) operator $C_n(C_n^{\dagger})$, such that $[C_n^{\dagger},C_n]=i\hbar$. $C_n(C_n^{\dagger})$ then defines the annihilation (creation) operator of a particle. Under this transformation it transforms to the usual tight-binding Hamiltonian of a particle moving on a ring of N sites. Parameters x_n then define the displacement of lattice points from their respective equilibrium positions. Although here we consider the local displacement of atoms (optical phonons), the collective motion of atoms in the lattice (acoustic phonon) can be incorporated in this formalism by making appropriate modifications of H.[48] Now from Hamilton's principle we find that

$$i\dot{C}_m=2\frac{\partial H}{\partial C_m^{\star}}=\omega_m(x_m)+C_{m+1}+C_{m-1} \tag{62}$$

$$\dot{x}_l=\frac{\partial H}{\partial p_l}=\frac{p_l}{m_l}, \tag{63}$$

and

$$-\dot{p}_l=\frac{\partial H}{\partial x_l}=\omega_l'(x_l)|C_l|^2+V_l'(x_l). \tag{64}$$

We now assume that the dynamical evolution of x_l occurs on a much longer time scale compared to the time scale of C_l. So the dynamics of the other system is determined primarily by the adiabatic variation of x_n.[7] In the electron lattice interaction language, the dynamics of the lattice is assumed to be far slower compared to the dynamics of the electron. Since the adiabatic approximation for x_l implies $\dot{p}_l=0$ for $l\in N$, the equation for determining x_l is then

$$\omega_l'(x_l)|C_l|^2=-V_l'(x_l). \tag{65}$$

Consider, for example, $V_l(x_l)=1/2k_lx_l^2$ and $\omega_l(x_l)=E_lx_l$. Then from Eq. (65) we obtain $x_l=(E_l/k_l)|C_l|^2$. Introduction of this into Eq. (62) yields the DNLSE's where $f_l(|C_l|)=|C_l|^2$ and $\chi_l=E_l^2/k_l$.

In principle $\omega_n(x_n)$ can be a nonlinear function of x_n. Furthermore, the overall dynamics of x_n can be quite complicated, and yet can be physically realistic. A few example in this regard have already been considered in the literature.[41–43,45] We consider a situation, where for $n\in N$, $V_n(x_n)$ is given by Eq. (59), and for $\omega(x)$ we assume

$$\omega(x)=\frac{E_0}{\gamma}\left(\frac{1-\cos(2\gamma x)}{4\gamma^2}\right)^{d-1}\sin(2\gamma x). \tag{66}$$

Then from Eq. (65) we obtain

$$\left[1-\delta^2\left(\frac{d-1}{d}\right)^2\left|C\right|^4\right]\tan^2(2\gamma x)-2\delta|C|^2\tan(2\gamma x)+\delta^2\left(\frac{2d-1}{d^2}\right)|C|^4=0, \tag{67}$$

where

$$\delta=\frac{4E_0\gamma}{k}=\frac{4E_0^2/k}{E_0/\gamma}=\frac{\chi}{\Delta}. \tag{68}$$

Equation (67) then yields

$$\tan(2\gamma x)=\frac{\delta|C|^2}{y}\left[1+\sqrt{\left(1-y\frac{(2d-1)}{d^2}\right)}^{1/2}\right] \tag{69}$$

where

$$y=1-\frac{\chi^2}{\Delta^2}\left(\frac{d-1}{d}\right)^2|C|^4. \tag{70}$$

Then for $d=1$ we have $y=1$. This in turn yields $\tan(2\gamma x)=\delta|C|^2$. Then, after some simple algebra, we obtain

$$\omega(x)=-\frac{\chi|C|^2}{\sqrt{1+\left(\frac{\chi}{\Delta}\right)^2|C|^4}}. \tag{71}$$

We consider next the other limit where $\gamma\to 0$. Then from Eq. (69) we obtain

$$x\approx\frac{2E_0}{k}(2d-1)|C|^2. \tag{72}$$

This in turn yields $\omega(x)=-\chi_\sigma|C|^\sigma$, where $\sigma=2(2d-1)$ and

$$\chi_\sigma=-\left[2^{d+2}\left|E_0\right|\left(\frac{|E_0|(2d-1)}{k}\right)^{2d-1}\right]. \tag{73}$$

Then for $d=1$, we obtain $\omega(x)=\chi|C|^2$. Introducing this into Eq. (62), we obtain the desired DNLSE.

We consider another model where we take $\omega(x)=2E_0x$, and $V(x)$ is given in Eq. (59). Then again from Eq. (65) we obtain

$$E_0|C|^2=-kd|x|^{2(d-1)}x. \tag{74}$$

This in turn yields

$$|x|=\left|\frac{E_0}{kd}\right|^{1/(2d-1)}|C|^{2/(2d-1)}. \tag{75}$$

Consequently we have $\omega(x)=-\tilde{\chi}(\sigma')|C|^\sigma$, where $\sigma'=2/(2d-1)$ and

$$\tilde{\chi}(\sigma')=2|E_0|\left|\frac{E_0}{kd}\right|^{1/(2d-1)}. \quad (76)$$

Then inserting $\omega(x)$ into Eq. (62), we obtain the desired set of equations.

VII. CONCLUSION

The formation of stationary states due to a single nonlinear impurity in a Caley tree and a dimeric nonlinear impurity in a perfect one-dimensional (1D) linear system are studied here using the DNLSE. Two types of nonlinear impurities—namely, $f(|C|)=|C|^{\sigma}$, where σ is arbitrary, and the rotational impurity are considered. Altogether four cases are studied. Important features of these problems are thoroughly discussed in the text. Whenever necessary, analytical arguments in support of numerical results are provided. Some important aspects of this paper are elucidated further below.

In this paper a very useful synthesis of the usual Green's function approach and the ansatz approach is made, to gain a better understanding of the problems. Because of synthesis we are able to derive many important results. For example, in the case of a nonlinear dimer with $f(|C|)=|C|^{\sigma}$, at $\sigma=2$ and $|\chi|>8/3$ a stationary localized state in which $|\phi_0|\neq|\phi_1|$ is obtained. However, for $\sigma=1,3$, and 4, no such χ_{cr} is found. So, it appears that, for this nonlinear dimer, $\sigma=2$ is a very special case. Of course, further analysis is required, and this will be presented elsewhere.

For the nonlinear dimer problem, $|\chi_{cr}|\sim 2$ and 3.6 have been reported in the literature. These values of $|\chi_{cr}|$ separate the whole of the $\sigma=2$ line into three regions, having no SL state, one SL state, and two SL states, respectively. On the other hand our analysis gives three values of $|\chi_{cr}|$, namely, 1, 8/3, and 8. Furthermore, from our analysis we do not find $|\chi_{cr}|\sim 3.6$. It is not clear from Ref. 40 what is the characteristic of the extra state that appears for $|\chi|\geq 3.6$. We also have a $|\chi_{cr}|$ at 8 separating two-SL-state and four-SL-state regions, with three SL states at that point.

For the monomer problem $|\chi_{cr}|=8$ does not exist. However, one obtains $|\chi_{cr}|=2$ which separates the no-SL-state and two-SL-state regions. The analytical reason behind this is discussed here. Furthermore, the equation for the critical line separating these regimes is analytically derived. In fact, equations describing various critical lines are derived from a general analytical approach. Our numerical results also agree very well with our analytical results. We further note that for the dimer problem this $|\chi_{cr}|$ is 1. So it appears that for a cluster of N sites, this $|\chi_{cr}|$ will go as $1/N$. This assertion, however, needs a thorough investigation.

Another interesting feature of this problem is the possibility of more localized states than the number of impurities in certain situations. This happens due to multiple permissible values of the amplitude at the impurity sites. Furthermore, the localization length of one set of states increases, while this length in the other set of states decreases as the strength of the nonlinearity parameter (χ) increases. Hence, in contrast to the static impurity case, the system here can assume more than one configuration.

Physically, the effect of localized states is manifested in transport properties of the material. However, a system containing a finite number of impurities can only produce a finite number of such states. So the probability that these states will exert their influence on transport properties of the system is very small, if not unlikely. On the other hand, for a thorough understanding of properties of a disordered system comprising nonlinear impurities and perfect sites, a critical understanding of these problems is essential. So the importance of the problems presented here should be understood in this context.

[1] T. D. Holstein, Ann. Phys. (N.Y.) **8**, 325 (1959); **8**, 343 (1989).

[2] A. S. Davydov, J. Theor. Biol. **38**, 559 (1973); Usp. Fiz. Nauk. **138**, 603 (1982) [Sov. Phys. Usp. **25**, 899 (1982)], and references therein.

[3] A. C. Scott, F. Y. Chu, and D. W. McLaughlin, Proc. IEEE **61**, 1443 (1973).

[4] J. C. Eilbeck, P. S. Lomdahl, and A. C. Scott, Physica D **16**, 318 (1985).

[5] J. M. Hyman, D. W. McLaughlin, and A. C. Scott, Physica D **3**, 28 (1981).

[6] D. W. Brown, K. Lindenberg, and B. J. West, Phys. Rev. B **37**, 2946 (1988).

[7] *Davydov's Soliton Revisited: Self Trapping of Vibrational Energy in Protein*, Vol. 243 of NATO Advanced Study Institute Series B: Physics, edited by Peter L. Christian and Alwyn C. Scott (Plenum, New York, 1991).

[8] D. Chen, M. I. Molina, and G. P. Tsironis, J. Phys. Condens. Matter **5**, 8689 (1993).

[9] Yi Wan and C. M. Soukoulis, Phys. Rev. B **40**, 12 264 (1989).

[10] Yi Wan and C. M. Soukoulis, Phys. Rev. A **41**, 800 (1990).

[11] V. M. Kenkre, Physica D **68**, 153 (1993).

[12] M. I. Molina and G. P. Tsironis, Phys. Rev. Lett. **73**, 464 (1994).

[13] M. Johansson, M. Hornquist, and R. Riklund, Phys. Rev. B **52**, 231 (1995).

[14] V. M. Kenkre and D. K. Campbell, Phys. Rev. B **34**, 4959 (1986).

[15] V. M. Kenkre and G. P. Tsironis, Phys. Rev. B **35**, 1473 (1987).

[16] V. M. Kenkre, G. P. Tsironis, and D. K. Campbell, in *Nonlinearity in Condensed Matter*, edited by A. R. Bishop, D. K. Campbell, P. Kumar, and S. E. Trullinger (Springer-Verlag, Berlin, 1987).

[17] G. P. Tsironis and V. M. Kenkre, Phys. Lett. A **127**, 209 (1988).

[18] V. M. Kenkre and G. P. Tsironis, Chem. Phys. **128**, 219 (1988).

[19] G. P. Tsironis, V. M. Kenkre, and D. Finley, Phys. Rev. A **37**, 4474 (1988).

[20] V. M. Kenkre and M. Kus, Phys. Rev. B **46**, 13 792 (1992).

[21] V. M. Kenkre and M. Kus, Phys. Rev. B **49**, 5956 (1994).

[22] V. M. Kenkre and P. Grigolini, Z. Phys. B **90**, 247 (1993).

[23] V. M. Kenkre and H. -L. Wu, Phys. Rev. B **39**, 6907 (1989).

[24] D. Hennig and B. Esser, Phys. Rev. A **46**, 4569 (1992).

[25] M. I. Molina and G. P. Tsironis, Physica D **65**, 267 (1993).

[26] P. Grigolini, H. -L. Wu, and V. M. Kenkre, Phys. Rev. B **40**, 7045 (1989).

[27] H. Wipf, A. Magerl, S. M. Shapiro, S. K. Satija, and W. Thimlinson, Phys. Rev. Lett. **46**, 947 (1981).

[28] A. Magerl, A. J. Dianoux, H. Wipf, K. Neumaior, and I. S. Anderson, Phys. Rev. Lett. **56**, 159 (1986).
[29] D. H. Dunlap, V. M. Kenkre, and P. Reineker, Phys. Rev. B **47**, 14 842 (1992).
[30] B. C. Gupta and K. Kundu, Indian J. Phys. A (to be published).
[31] P. K. Dutta and K. Kundu, Phys. Rev. B **53**, 1 (1996).
[32] S. Takeno and S. Homma, J. Phys. Soc. Jpn. **60**, 731 (1991).
[33] Y. S. Kivshar, Phys. Rev. B **47**, 11 167 (1993).
[34] Y. S. Kivshar, Phys. Lett. A **161**, 80 (1991).
[35] D. Cai, A. R. Bishop, and N. Gronbech-Jensen, Phys Rev. Lett. **72**, 591 (1994).
[36] D. Hennig, K. O. Rasmussen, G. P. Tsironis, and H. Gabriel, Phys. Rev. E **52**, R4628 (1995).
[37] M. J. Ablowitz and J. M. Ladik, J. Math. Phys. **17**, 1011 (1976).
[38] R. Scharf and A. R. Bishop, Phys. Rev. A **43**, 6535 (1991).
[39] M. Johansson and R. Riklund, Phys. Rev. B **49**, 6587 (1994).
[40] M. I. Molina and G. P. Tsironis, Phys. Rev. B **47**, 15 330 (1993).
[41] G. P. Tsironis, M. I. Molina, and D. Hennig, Phys. Rev. E **50**, 2365 (1994).
[42] Y. Y. Yiu, K. M. Ng, and P. M. Hui, Phys. Lett. A **200**, 325 (1995).
[43] Y. Y. Yiu, K. M. Ng, and P. M. Hui (unpublished).
[44] D. Cassi, Europhys. Lett. **9**, 627 (1989).
[45] V. M. Kenkre, H. -L. Wu, and I. Howard, Phys. Rev. B **51**, 15 841 (1995).
[46] E. N. Economou, *Green's Function in Quantum Physics* (Springer-Verlag, Berlin, 1983).
[47] H. Goldstein, *Classical Mechanics* (Addison-Wesley Reading, MA, 1950), p. 290.
[48] G. Kalosakas, G. P. Tsironis, and E. N. Economou, J. Phys. Condens. Matter **6**, 7847 (1994).